European Polymer Journal 180 (2022) 111597

Contents lists available at ScienceDirect

European Polymer Journal

journal homepage: www.elsevier.com/locate/europolj

Effect of gelatin concentration, ribose and glycerol additions on the electrospinning process and physicochemical properties of gelatin nanofibers

Alaitz Etxabide [a,b,*], Alireza Akbarinejad [c,d], Eddie W.C. Chan [c,d], Pedro Guerrero [a,e], Koro de la Caba [a,e], Jadranka Travas-Sejdic [c,d], Paul A. Kilmartin [b]

[a] BIOMAT Research Group, University of the Basque Country (UPV/EHU), Escuela de Ingeniería de Gipuzkoa, Plaza de Europa 1, 20018 Donostia-San Sebastián, Spain
[b] School of Chemical Sciences, The University of Auckland, Private Bag 92019, Auckland, New Zealand
[c] Polymer Biointerface Centre, School of Chemical Sciences, The University of Auckland, 23 Symonds Street, Auckland, New Zealand
[d] MacDiarmid Institute for Advanced Materials and Nanotechnology, PO Box 600, Wellington, New Zealand
[e] BCMaterials, Basque Center for Materials, Applications and Nanostructures, UPV/EHU Science Park, 48940 Leioa, Spain

ARTICLE INFO

Keywords:
Gelatin
Electrospinning
Fibres
Maillard reaction
Physical crosslinking

ABSTRACT

Rheological properties of gelatin-based solutions containing different concentrations of ribose and/or glycerol were assessed before electrospun mats were manufactured and their properties investigated. Characterization included morphology, X-ray diffraction, Fourier transform infrared, solubility, swelling, the release of Maillard reaction (MR) products and their antioxidant activity. Gelatin concentrations ≥ 16 % w/v favoured the formation of smooth nanofibres in the electrospinning process due to their higher viscosity than for gelatin concentrations ≤ 14 % w/v. The diameters of the nanofibres were between 300 and 400 nm, irrespective of the concentration of gelatin and the additives. Heat treatments (80–110 °C) of the samples induced MR between gelatin and ribose, which provided the mats with water stability. Nevertheless, the fibrous morphology only remained for those mats heat-treated at 110 and 100 °C and containing 10 and 20 wt% ribose, respectively, after sample immersion in water. Heat treatment at 110 °C, along with glycerol addition, resulted in a decrease of solubility (from 100 to ~ 9 %) and provided a water absorption capacity (1,500–2,500 %), due to the crosslinking of ribose and glycerol with gelatin. Release of MR antioxidant compounds from the mats into water exhibited DPPH radical scavenging activity values up to 38 % (0.61 GAE μg/mL).

1. Introduction

Solution electrospinning is a well-established, simple, cost-effective and flexible technique that produces continuous solid fibres from a polymer solution using electrostatic forces. Many parameters can influence the electrospinning process, including solution properties (e.g., formulation, polymer concentration, viscosity, surface tension), electrical field strength, solution flow rate, distance to the collector plate, humidity and temperature, among others [1]. Electrospun nanofibres exhibit characteristics such as large surface area per unit mass, high porosity, small interfibrous pore size, and high gas permeability. These properties make them of interest to textile, agricultural, water treatment, air filtration, energy storage, cosmetic, electronic and sensors, pharmaceutical, biomedical, and packaging applications, among others [2,3].

Different types of materials, including both synthetic and natural polymers and their combinations, can be used to obtain fibres *via* solution electrospinning. Among these polymeric materials, synthetic polymers, such as polystyrene and poly(vinyl chloride), biocompatible and biodegradable synthetic polymers, such as poly(lactic acid) and poly (lactic-*co*-glycolic acid), conducting polymers, such as polyaniline and polypyrrole, and natural polymers, such as chitosan, alginate, collagen and gelatin, have been directly electrospun into nanofibres [4–9]. Some of the most commonly used solvents are alcohols, dichloromethane, chloroform, dimethylformamide, tetrahydrofuran, acetone, dimethyl sulfoxide, hexafluoroisopropanol and trifluoroethanol [4]. There has

* Corresponding author at: BIOMAT research group, University of the Basque Country (UPV/EHU), Escuela de Ingeniería de Gipuzkoa, Plaza de Europa 1, 20018 Donostia-San Sebastián, Spain.
E-mail address: alaitz.etxabide@ehu.es (A. Etxabide).

https://doi.org/10.1016/j.eurpolymj.2022.111597
Received 22 March 2022; Received in revised form 13 September 2022; Accepted 21 September 2022
Available online 26 September 2022

been an increasing interest in using non-toxic and more environmentally friendly materials and solvents in recent years. These include renewable biopolymers and water-based solvents, which are greener options compared to synthetic polymers and toxic solvents [10].

Among the water-soluble natural polymers, gelatin is a protein from biological origin, with high biodegradability, biocompatibility, water absorbability, non-immunogenicity and commercial availability. Owing to these properties, gelatin in various forms (e.g., films, scaffolds, capsules, filters) has been used in cosmetics, pharmaceutical, medical, food and water filtration applications [3]. However, due to the hydrophilic nature of gelatin, stabilization of its structure is required, since, without any stabilization of the biopolymer, gelatin-based materials generally dissolve and lose their structure.

Among the methods available for gelatin structure stabilization, protein crosslinking is one of the most widely used strategies to achieve hydrolytic stability of gelatin-based samples [11]. In this matter, crosslinkers such as glutaraldehyde and genipin have been widely used. However, there are potential toxicity problems, as well as the requirement of intensive detoxifying strategies related to residual unreacted glutaraldehyde groups, while the high cost of genipin is a major drawback when using these crosslinkers [11,12]. To eliminate toxicity risks and provide cost-effectiveness, the heat treatment of gelatin with sugar molecules has been introduced as an alternative chemical crosslinking method [13,14]. This condensation reaction between proteins and sugar is known as the Maillard reaction (MR).

The properties of gelatin-based materials (e.g., solubility, swelling, antioxidant activity, morphology preservation after immersion) are dependent on the extent of the MR, which, in turn, depends on parameters such as the type of sugar, reaction time and temperature, and the pH of the solution. Pentoses (e.g., ribose) are a more reactive crosslinker than hexoses (e.g., glucose) and disaccharides (e.g., lactose) [15–17], while an increase in sugar percentage (up to a certain point), temperature or pH of the solution induces a more extended reaction [18,19]. Additionally, glycerol has been added as a plasticizer to improve material's processability.

In this study, gelatin-based solutions with different amounts of gelatin and ribose (chemical crosslinker) and glycerol (plasticizer, physical crosslinker) were prepared to analyse their rheological properties before electrospinning. After producing gelatin-based fibres, the samples were characterized according to their morphology and fibre size. Different temperatures were used to induce the MR and crosslink the samples. Heat-treated samples were assessed regarding their morphology preservation after immersion in water as a function of their composition and heat treatment. Finally, a specific heat treatment temperature was selected and the physicochemical properties of the samples were further analysed using X-ray diffraction, Fourier transform infrared spectroscopy, swelling, solubility, the release of MR compounds and their antioxidant properties.

2. Materials and methods

2.1. Materials

A commercial type A codfish gelatin (Weishardt International, Liptovsky Mikulas, Slovakia) was employed as a matrix. The gelatin had a Bloom value of 200, 11.06 % moisture and 0.147 % ash. Ribose and glycerol (ECP LabChem) were used as a crosslinker and a plasticizer, respectively. Mili-Q water (MQW) was used as the solvent. 2,2-diphenyl-1-picryl hydrazyl (DPPH) and gallic acid were purchased from Sigma-Aldrich, while methanol was obtained from ECP LabChem (Auckland, New Zealand).

2.2. Preparation of gelatin-based solutions

To analyse the effect of gelatin concentration on the rheological properties of the gelatin-based solutions, 10, 12, 14, 16, 18 and 20 % w/v gelatin solutions [3] were prepared by mixing gelatin with 5 mL MQW under stirring at 250 rpm and 60 °C for 30 min. To assess the effect of ribose and/or glycerol addition (10 and 20 wt% on gelatin dry basis) on the rheological properties of the gelatin solutions, 20 % w/v gelatin concentration was chosen, given the formation of smooth, bead-free nanofibres at this concentration with higher amounts of gelatin electrospun per minute. The chemicals were mixed with 5 mL MQW and the solution was then stirred at 250 rpm and 60 °C for 30 min. The samples are named as follows: xGexRixGly where x is the concentration, and Ge, Ri and Gly mean gelatin, ribose and glycerol, respectively.

2.3. Rheological properties of gelatin-based solutions

For all rheological measurements, a Modular Compact Rheometer-MCR 302 (Anton Paar) with a stainless steel measuring plate PP50 (ø 50 mm) was used. The temperature was controlled using a water bath (Julaba F 12). 1.5 mL of the gelatin solution was placed in the stationary plate and the gap between plates was set as 0.3 mm. For each rheological characterisation, a fresh solution was prepared and a minimum of two replicates (n = 2) was assessed for each formulation [20].

2.3.1. Temperature sweep: Oscillatory test for storage and loss moduli measurements

Temperature sweeps from 34 to 18 °C and 18 to 34 °C, with cooling/heating rates of 0.5 °C/min, were conducted. The values of storage modulus (G') and loss modulus (G'') were determined at 0.5 % strain and 1 Hz frequency. The crossover point of G' and G'' during cooling and heating was considered as gelling (Tgel) and melting (Tmel) temperature of the solution, respectively.

2.3.2. Temperature sweep: Rotational test for apparent viscosity measurements

A temperature sweep from 34 to 18 °C, with a cooling rate of 0.5 °C/min, was conducted to analyse the viscosity of the gelatin-based solutions, using a rotational test and a constant shear rate of 6.39 s^{-1}. The shear rate (ɣ) was determined as a function of the needle (21G, inner diameter of 0.51 mm) and flow rate (Q, 0.3 mL/h), used in preliminary electrospinning trials using the following equation (1):

$$\gamma = \frac{4Q}{\pi R^3} \tag{1}$$

where Q is the flow rate and R is the inner radio (mm) of the needle.

2.3.3. Shear rate sweep: Rotational test for viscosity measurements

A shear rate sweep from 1 to 1000 s^{-1} was conducted to analyse the viscosity of gelatin solutions (10Ge-20Ge) using a rotational test and at constant temperature (Tgel and Tmel). The obtained data were fitted to the Carreau-Yasuda rheological model using Origin software to estimate the viscosity in a non-Newtonian fluid [21]:

$$\eta(\dot{\gamma}) = \dot{\eta}(\infty) + (\eta(0) - \eta(\infty))[1 + (\lambda\dot{\gamma})^a]^{\frac{n-1}{a}} \tag{2}$$

2.4. Preparation of gelatin mats

Gelatin-based solutions were prepared as indicated above (Section 2.2) and transferred to 5 mL plastic syringes. The syringe was placed in the syringe pump (Adelab Scientific), which was inside the electrospinning chamber, previously conditioned at 30.7 °C ± 0.6 and 29 % ± 2 RH. The temperature of the solution was kept steady to homogenize for 30 min before electrospinning. This temperature was set to avoid another variable in the electrospinning process, and considering that: i) electrospinning of gelatin can be realized only from solutions in which gelatin adopts a random coil conformation (T > Tgel) [22]; ii) formation of droplets was avoided; iii) all formulations (10Ge-20Ge) produced fibres (preliminary tests). The solution was then electrospun under an applied voltage of 22 kV (Bertan 230) across a fixed distance of 15 cm

between the tip of the needle (21G) and the rotational (5.71 rpm) flat stainless-steel (ø 10 cm) collector covered with aluminium foil. A controlled feeding rate of 0.3 mL/h was employed for 15 min for fibre size analysis (n = 2) and 210–240 min for gelatin-based mat preparation (n ≥ 3).

2.5. Morphology of gelatin mats

The samples were fixed on glass slides using carbon tapes and sputter-coated with gold (10 nm) using a sputter coater (Quorum Q150R S). A scanning electron microscope (SEM, JCM-6000 Versatile Benchtop SEM) was used to observe the morphology of mats at an accelerating voltage of 15 kV and a magnification of ≥ 800 ×. For fibre size evaluation, ImageJ software was used, taking at least 5 SEM images, and at least 180 measurements were undertaken on 15-min electrospun fibre samples.

2.6. Heat-treatment effect on the morphology of gelatin mats after immersion in water

Samples prepared with 20 % w/v gelatin concentration for 210–240 min, producing smooth nanofibres and with higher amounts of gelatin electrospun per minute, were peeled off, heat-treated (HT) at 80, 90, 100, and 110 °C for 24 h to induce crosslinking between gelatin and ribose, and immersed in MQW at 37 °C for 24 h. The samples were then taken out from MQW and left to dry in an air-circulating fume hood at room temperature (20 °C) for 24 h. The morphology of the HT samples was analysed before and after immersion using SEM as explained above (section 2.5). The heat treatment temperature is indicated as follows: xHT, where x is the temperature (°C).

2.7. Characterization of mats

2.7.1. X-ray diffraction (XRD)

X-ray diffraction studies of gelatin-based mats were performed with a diffraction unit (Empyrean, Malvern Panalytical, Cleveland, New Zealand) operating at 45 kV and 40 mA. The radiation was generated from a Cu-Kα (λ = 1.5418 Å) source. The diffraction data of the samples were collected at 2θ values from 5° to 30°, where θ is the incidence angle of the X-ray beam on the sample [23].

2.7.2. Attenuated total reflection-Fourier transform infrared (ATR-FTIR) spectroscopy

FTIR spectra of mats were carried out on a Bruker Vertex 70 FTIR spectrometer using a single bounce Platinum Diamond Micro-ATR accessory (Bruker Optics, New Zealand). A total of 32 scans were performed at 4 cm^{-1} resolution and the measurements were recorded between 4000 and 750 cm^{-1} (n = 4).

2.7.3. Swelling

The swelling was calculated gravimetrically under physiological temperature. Three specimens (n = 3) of each mat were weighed (W_o) and immersed in 3.5 mL of MQW. The flasks were stored in an oven at 37 °C for 24 h. The samples were then removed from the solutions, drip-dried for 5 s and reweighed (Wt) [14]. Swelling (Sw) was calculated using the following equation:

$$Sw(\%) = \frac{(W_t - W_o)}{W_o} \times 100 \quad (3)$$

2.7.4. Solubility

Three specimens (n = 3) of each mat were weighed (W_o) and immersed in 3.5 mL of MQW. The flasks were stored in an oven at 37 °C for 24 h. The specimens were taken out and left to dry in an air-circulating fume hood at room temperature (20 °C) for 24 h before reweighing (Wt) [14]. The solubility (S) of mats was calculated using the following equation:

$$S(\%) = \frac{(W_o - W_t)}{W_o} \times 100 \quad (4)$$

2.7.5. Release of MR compounds and their antioxidant activity

The release of MR products from mats into MQW was analysed by immersing the mats (3.38 ± 0.21 mg) in 3.5 mL of MQW at 37 °C for 24 h. The specimens were then taken out of MQW,the liquid was introduced into quartz cuvettes and analysed on a NanoPhotometer (NP80, IMPLEN) by recording absporption intensity at wavelengths from 200 to 400 nm. Three mats (n = 3) were analysed for each composition.

DPPH radical scavenging activity was measured on the liquid samples (n = 3) obtained after the release test. 2 mL of the solution was mixed with 2 mL of DPPH solution (150 μM) in methanol. The mixture was vigorously shaken and allowed to stand at room temperature in the dark for 30 min [24]. Free radical scavenging activity of samples was expressed as μg/mL gallic acid equivalent (GAE, calibration curve (0.125–1.25 μg/mL): y = 2.34 + 59.77x, R^2 0.999). The inhibition values were determined by the absorbance decrease at 517 nm as follows:

$$\text{Inhibition}\,(\%) = \frac{(A_c - A_s)}{A_c} \times 100 \quad (5)$$

where A_c is the absorbance of the MQW where 20Ge mats (control sample) were immersed, and A_s is the absorbance of the MQW where other mats were immersed.

2.8. Statistical analysis

Data were subjected to one-way analysis of variant (ANOVA) using an SPSS computer program (SPSS Statistic 25.0). Post hoc multiple comparisons were determined by Tukey's test with the level of significance set at $P < 0.05$.

3. Results and discussion

3.1. Rheological properties of gelatin-based solutions

Fig. 1 **a-c** and Table 1 clearly show the influence of gelatin concentration on the melting and gelling properties of the gelatin solutions, as well as on their flow behaviour and viscosity. As the concentration of gelatin increased, Tmel and Tgel shifted to higher values (Table 1). The gelatin concentration showed a stronger influence on Tgel than on Tmel, as reported in the literature [20]. More gelatin could lead to higher protein–protein and protein-solvent interactions, which required higher temperatures to i) break the interactions down, increasing the Tmel, and ii) form bonds, increasing the Tgel. At these temperatures, gelatin behaved like a non-Newtonian fluid (Fig. 1**b**), especially at high shear rates, since the experimental data satisfactorily fitted ($R^2 > 0.986$ for Tgel; $R^2 > 0.998$ for Tmel) the Carreau-Yasuda model (Equation (2)), as shown in Tables 1S and 2S. Unlike gelatin concentration (from 10 to 20 % w/v), the behaviour of the fluids as a function of shear rate was temperature-dependent, as the viscosity of samples decreased with the increase in shear rate (shear-thinning) at Tgel, while it slightly increased (shear-thickening) at Tmel. The decrease in viscosity at Tgel can be related to the disentanglement of polymer chains, protein–protein and protein-solvent interactions with the increase in shear rate. The increase in viscosity at Tmel can be related to polymer chain stretching and alignment, which lead to the formation of intermolecular forces [25].

Regarding the temperature effect on the viscosity of gelatin solutions (Fig. 1**c**), the increase in gelatin concentration, and thus in gel reinforcement, notably increased the viscosity (at $\dot{\gamma}$=6.39 s^{-1}) of the solutions, as seen in Fig. 1**b**. As expected, the viscosity increased with a decrease in temperature. It is worth mentioning that the sudden increase in viscosity at temperatures close to the gelling point (21–24 °C, Table 1)

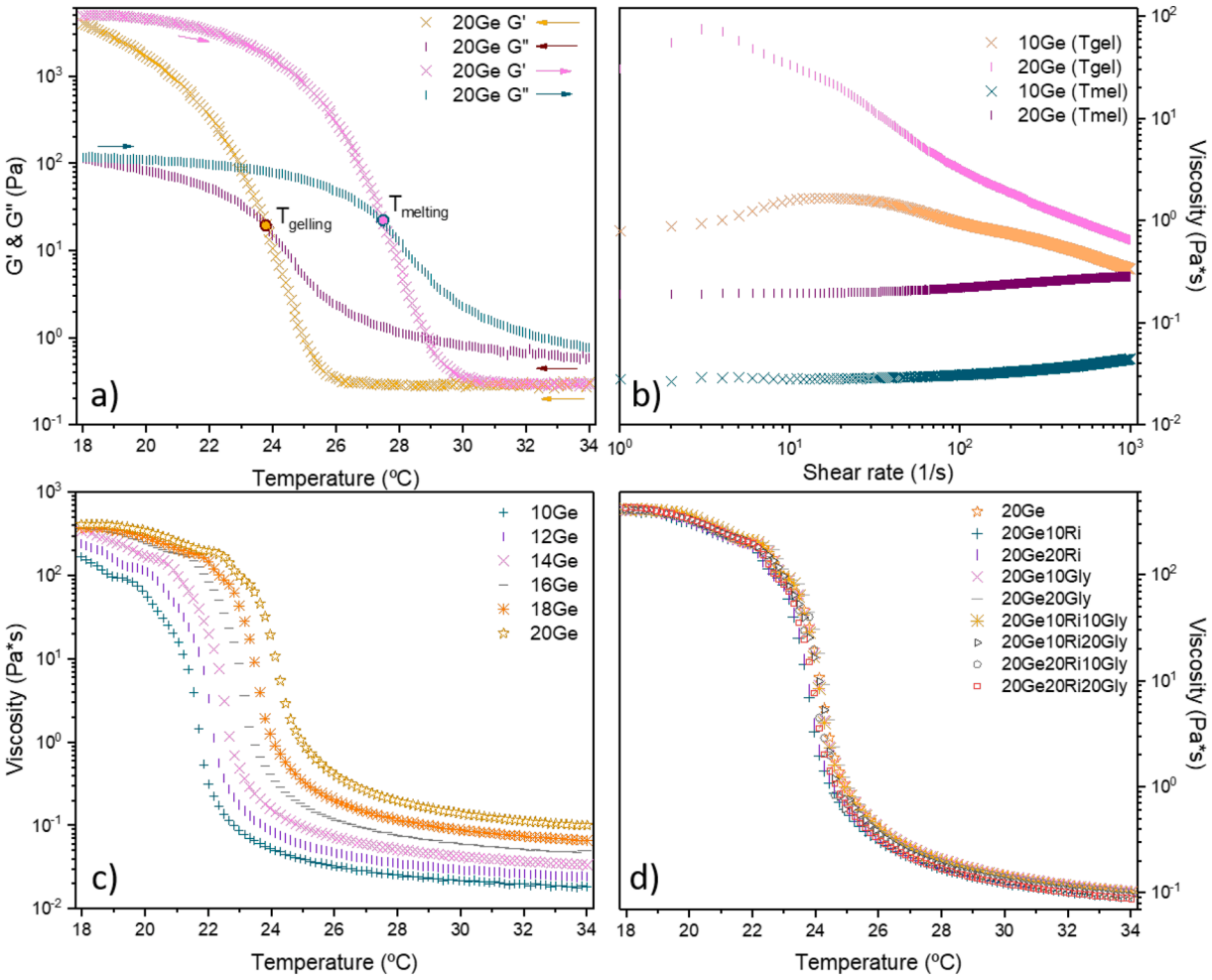

Fig. 1. a) Storage modulus (G') and loss modulus (G'') for 20 % w/v gelatin solution (20Ge) as a function of temperature (cooling (←) and heating (→)); b) viscosity values of 10 and 20 % w/v gelatin solutions (10Ge and 20Ge) as a function of shear rate and temperature (gelling temperature (Tgel) and melting temperature (Tmel)); and viscosity (γ=6.39 s^{-1}) values as a function of temperature; and c) gelatin (Ge) concentration (from 10 to 20 % w/v) and d) ribose (Ri) and/or glycerol (Gly) content (10 and 20 wt% on gelatin dry basis) (n = 2).

Table 1
Gelling and melting temperatures (Tgel and Tmel, respectively), as well as viscosity values (γ=6.39 s^{-1}) of gelatin-based solutions, for electrospinning at 30.7 ± 0.6 °C, as a function of gelatin (Ge) concentration (from 10 to 20 % w/v) and ribose (Ri) and/or glycerol (Gly) content (10 and 20 wt% on gelatin dry basis) (n = 2).

Gelatin solution (% w/v)	Tgel (°C)	Tmel (°C)	Viscosity 10^{-2} (Pa*s) at 30.7 ± 0.6 °C
10Ge	21.44 ± 0.02	26.10 ± 0.04	1.88 ± 0.21
12 Ge	21.73 ± 0.01	26.23 ± 0.02	2.69 ± 0.13
14 Ge	22.26 ± 0.03	26.53 ± 0.01	3.83 ± 0.19
16 Ge	22.83 ± 0.01	26.88 ± 0.01	5.70 ± 0.05
18 Ge	23.15 ± 0.02	27.08 ± 0.02	7.97 ± 0.33
20 Ge	23.75 ± 0.03	27.50 ± 0.04	13.08 ± 0.16
20Ge10Ri	23.43 ± 0.00	27.24 ± 0.00	11.83 ± 0.25
20Ge20Ri	23.48 ± 0.01	27.33 ± 0.02	12.46 ± 0.17
20Ge10Gly	23.75 ± 0.01	27.54 ± 0.00	13.33 ± 0.19
20Ge20Gly	23.95 ± 0.00	27.76 ± 0.01	12.64 ± 0.24
20Ge10Ri10Gly	23.76 ± 0.03	27.57 ± 0.04	13.30 ± 0.19
20Ge10Ri20Gly	23.84 ± 0.04	27.58 ± 0.03	13.43 ± 0.21
20Ge20Ri10Gly	23.74 ± 0.05	27.53 ± 0.05	13.39 ± 0.23
20Ge20Ri20Gly	23.75 ± 0.05	27.55 ± 0.04	13.50 ± 0.28

is related to the coil-to-helix transition and the formation of a molecularly ordered network induced by intra- and inter-molecular physical interactions [26]. Regarding the melting point, Gornall and Terentjev [27] reported that an increase in Tmel could be related to an increase in the stability of the triple helix which provided higher thermal stability to the gelatin solution.

The addition of ribose and glycerol into the gelatin formulations (Fig. 1**d**) did not have the same effect on the rheological properties as gelatin concentration. This is seen in the minor variation of Tgel, Tmel and viscosity values, compared to the gelatin solution with no additives (control sample, 20Ge) (Table 1). The small variations can be related to changes in the concentrations due to additive presence, as well as changes in physical crosslinks such as hydrogen bonds formed between gelatin and the additives [28].

3.2. *Morphological properties of gelatin-based mats*

The increase in gelatin concentration prevented the occurrence of beads in the electrospinning process, for gelatin solutions electrospun at 30.7 °C, 29 % RH, 22 kV and 0.3 mL/h (Fig. 2). Mats produced from gelatin concentrations up to 14 % w/v presented lots of beads while the use of gelatin solutions with concentrations equal to or higher than 16 % w/v favoured the formation of smooth, bead-free nanofibres. Similarly, Okutan and coworkers observed that gelatin solutions at 7 % w/v did not produce nanofibres, whereas regular nanofibre formation occurred with a 20 % w/v gelatin concentration [3]. Electrospinning of solutions with higher concentrations and viscosities (Table 1), resulted in an improvement in the viscoelastic forces. Hence, the partial breakup of the

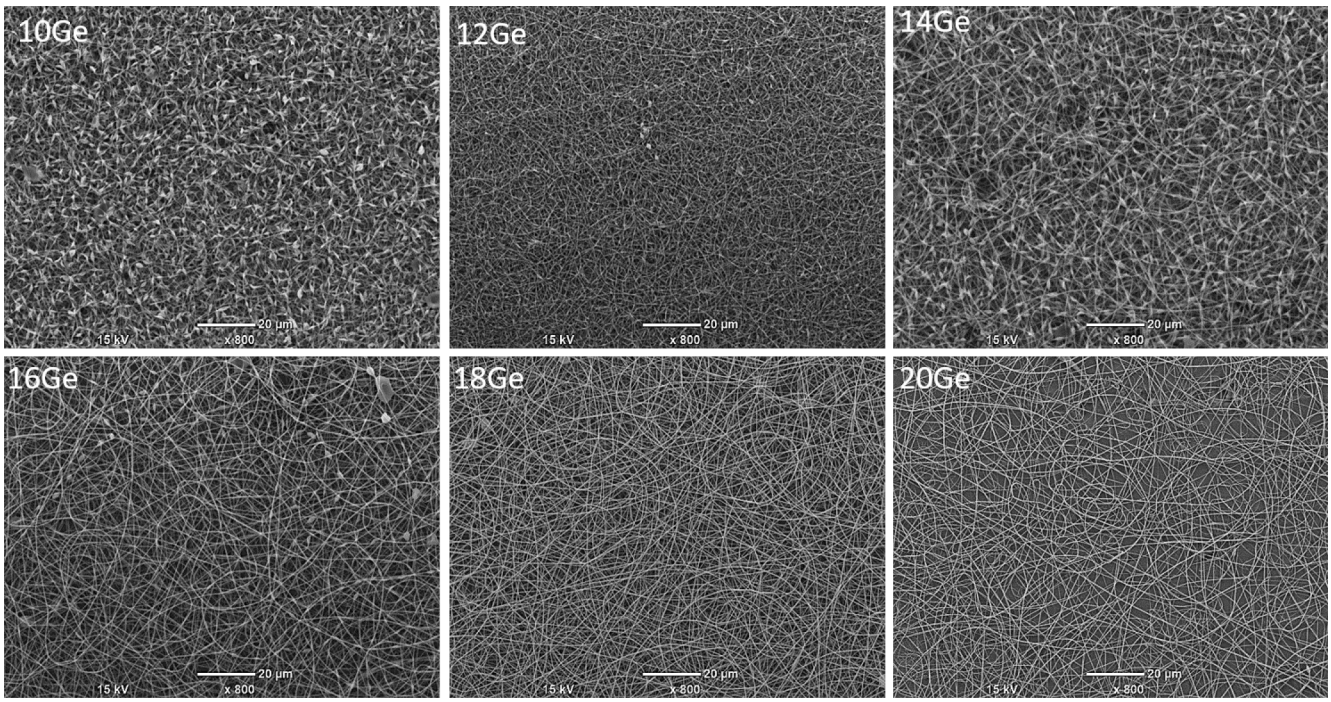

Fig. 2. SEM images of gelatin (Ge) mats as a function of gelatin concentration (from 10 to 20 % w/v).

polymer jet and the formation of beads is prevented, enabling the formation of smooth and uniform fibres [22,29]. The addition of ribose and glycerol did not alter the morphology of the mats (Fig. 3), irrespective of their percentages, resulting in the formation of smooth, bead-free nanofibres.

With regard to the size distribution of the nanofibres (Fig. 4**a**), the diameters were mainly between 300 and 400 nm, with a lesser percentage between 200 and 300 nm, irrespective of the gelatin concentration (16, 18 and 20 % w/v). The addition of ribose and glycerol (Fig. 4**b**), however, resulted in an increased percentage of nanofibres in the 400–500 nm range, although the main size range was still around 300–400 nm. Overall, the average nanofibre diameter slightly increased when ribose and glycerol were added (Table 2). Kawak and colleagues observed that the average diameter of the sugar-crosslinked gelatin nanofibres (in the 200–300 nm range) increased slightly when sugars were added [12]. Similarly, Siimon and coworkers showed that the average fibre diameters of pure gelatin nanofibres (between 280 and 575 nm) started to increase with the addition of glucose (> 5 %) [30]. This increase in fibre diameter was related to a higher concentration of solid material (gelatin + additives) in the formulation, which led to a slight increase in viscosity (Table 1). Although the viscosity of the solution is usually considered to be the dominant parameter which decides fibre diameter, the observed increase in fibre diameters might also be related to a possible decrease in conductivity of the biopolymer solution [31].

3.3. Heat-treatment effect on the morphology of gelatin-based mats after immersion

Unlike the gelatin-based mats without sugar (20Ge, 20Ge10Gly, 20Ge20Gly), the ribose-containing mats were not water-soluble, irrespective of glycerol content and the temperature used in the heat treatment (from 80 to 110 °C). This water stability improvement was related to the temperature-induced crosslinking *via* MR between the

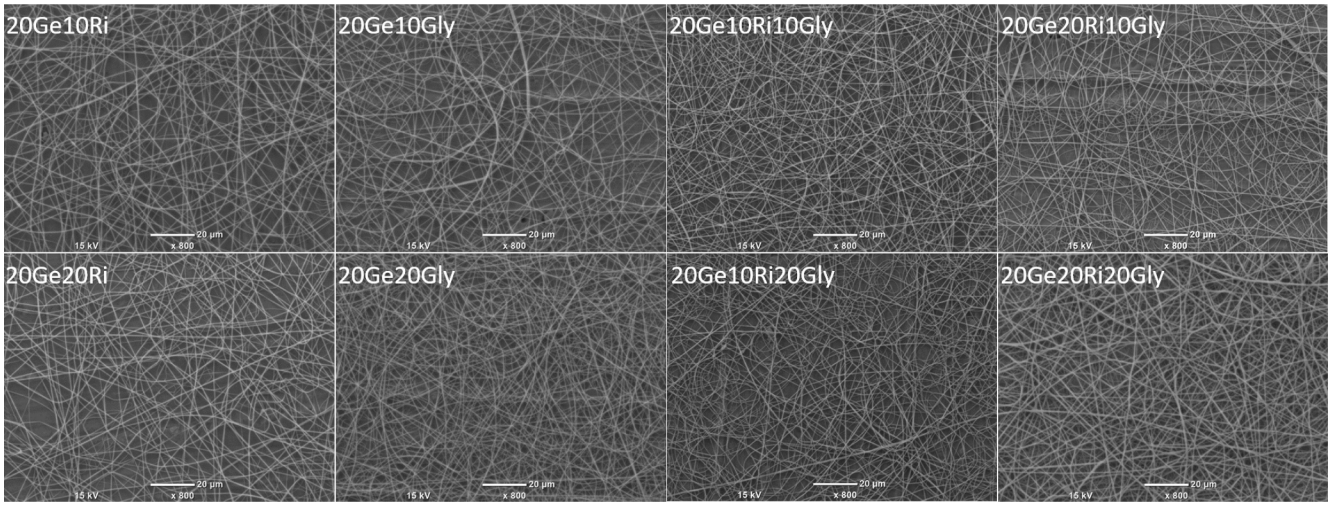

Fig. 3. SEM images of 20 % w/v gelatin (20Ge) mats as a function of ribose (Ri) and glycerol (Gly) content (10 and 20 wt% on gelatin dry basis).

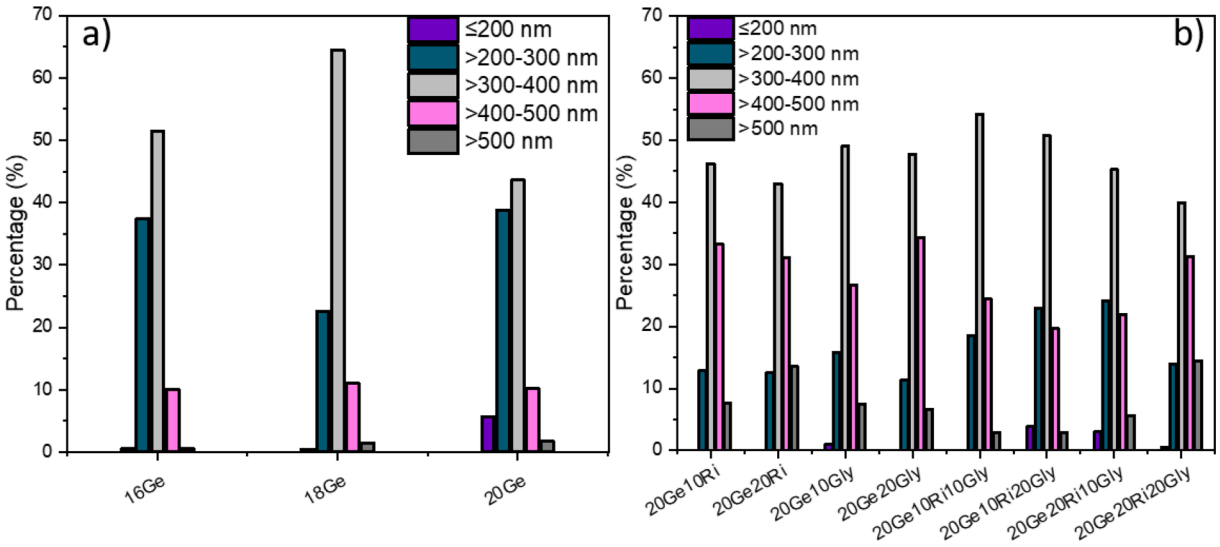

Fig. 4. Size distribution of fibres of a) gelatin (Ge) mats as a function of concentration (from 16 to 20 % w/v), and b) 20 % w/v (20Ge) mats as a function of ribose (Ri) and glycerol (Gly) content (10 and 20 wt% on gelatin dry basis) (n ≥ 180).

Table 2
Average fibre diamter of gelatin (Ge) mats as a function of gelatin concentration (from 10 to 20 % w/v), and ribose (Ri) and glycerol (Gly) content (10 and 20 wt% on gelatin dry basis) (n ≥ 180).

Gelatin mats	Fibre diameter (nm)
10Ge	-*
12Ge	-*
14Ge	-*
16Ge	324.5 ± 59.6
18Ge	344.5 ± 55.4
20 Ge	319.5 ± 80.3
20Ge10Ri	390.5 ± 80.3
20Ge20Ri	400.0 ± 92.4
20Ge10Gly	380.5 ± 84.8
20Ge20Gly	391.7 ± 77.4
20Ge10Ri10Gly	364.9 ± 71.1
20Ge10Ri20Gly	351.2 ± 77.3
20Ge20Ri10Gly	352.6 ± 79.3
20Ge20Ri20Gly	400.1 ± 92.7

*High presence of beads.

gelatin and ribose [19]. However, although crosslinked mats became more water-stable, the fibrous morphology of the mats was compromised, which was dependent on the crosslinker (ribose) concentration and heating temperature (Fig. 5 and Fig. 6). Fibre fusion happened after the immersion of mats heat-treated at temperatures ≤ 100 and ≤ 90 °C in mats containing 10 and 20 wt% ribose, respectively, resulting in film-like morphologies. At higher temperatures, the fibrous morphology remained, although the fusion of fibres still occurred. This was also observed by Kwak and colleagues in a study of electrospun gelatin mats crosslinked with sucrose, glucose or fructose [12], related to the extent of the MR. Stevenson and colleagues studied the addition of ribose into gelatin film-forming solutions and the subsequent heat treatment of films to promote the MR. It was concluded that a greater crosslinking extension occurred at the highest heating temperature (studied temperatures: room temperature, 70 and 90 °C) [19]. It is known that the MR is promoted at higher temperatures and prolonged heating, as well as with an increase (up to a certain concentration) of the crosslinker content [15,19,23]. Regarding the plasticiser addition, the presence of glycerol might play a minor role in the preservation of fibres, since glycerol induces the formation of hydrogen bondings between the protein and the plasticizer itself [32], which could help maintain the

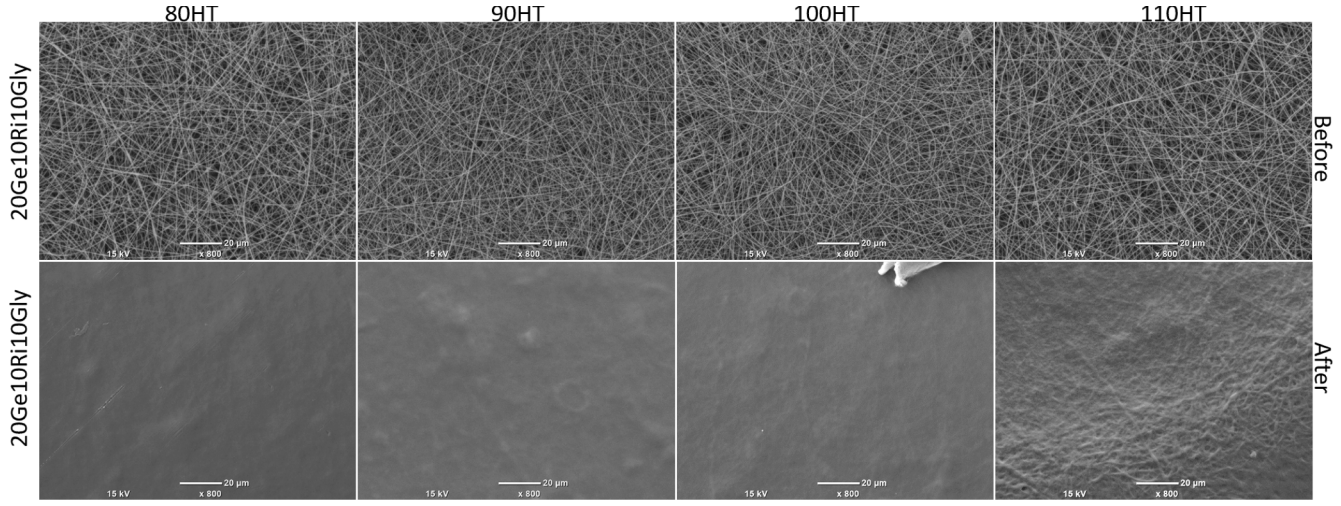

Fig. 5. SEM images of 20 % w/v gelatin (20Ge) mats with 10 wt% of both ribose (20Ri) and glycerol (10Gly) before and after immersion in MQW water at 37 °C for 24 h.

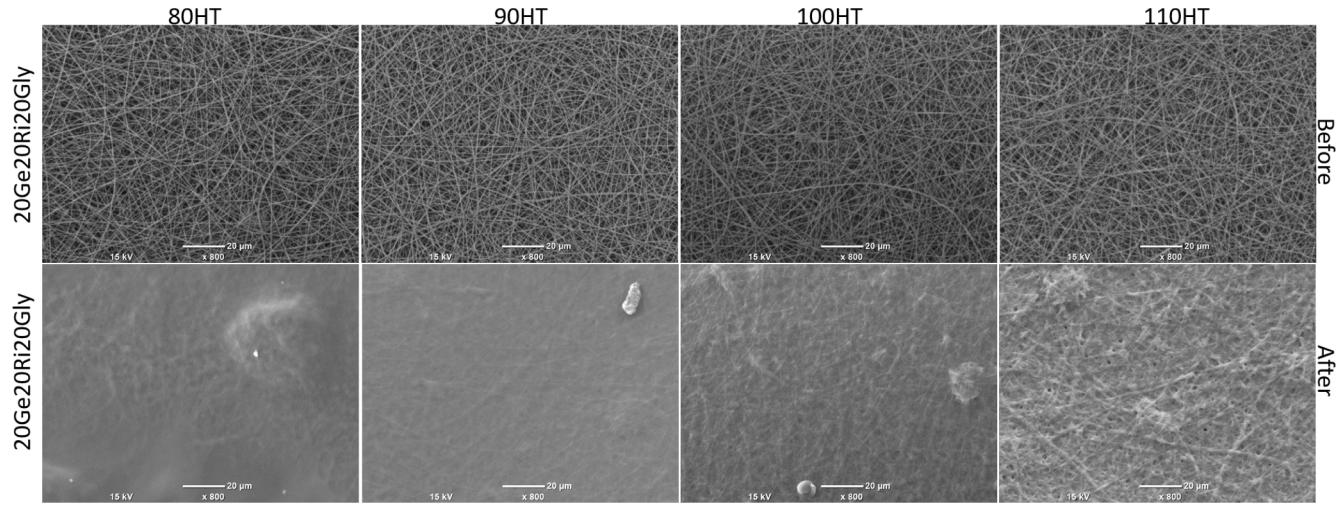

Fig. 6. SEM images of 20 % w/v gelatin (20Ge) mats with 20 wt% of both ribose (20Ri) and glycerol (20Gly) before and after immersion in MQW water at 37 °C for 24 h.

structure of the ribose-crosslinked mats.

3.4. Physicochemical characterization of mats heat-treated at 110 °C

XRD results indicated that the gelatin mats had an amorphous structure (Fig. 7), confirmed by the lack of peaks at 7.5° and 20° (2θ), associated with the residual triple-helix from native collagen and the partial crystalline structure of gelatin, respectively [33]. This can be attributed to fast water evaporation and, thus insufficient time to provide mobility to form ordered structures (e.g., hindering the renaturation of the triple-helix) during gelatin fibre formation and sample drying [22]. However, the intensity of the peaks slightly increased when both ribose and glycerol were present together in the formulation. This could be related to a more ordered biopolymer structure due to both the formation of new physical and chemical bonds between glycerol and ribose with gelatin, respectively. Morsy and colleagues observed similar XRD patterns with glycerol-containing and glucose-crosslinked gelatin electrospun mats [32].

FTIR spectra of all gelatin mats mostly presented the main characteristic vibrational bands belonging to gelatin (Fig. 8**a**): C═O stretching

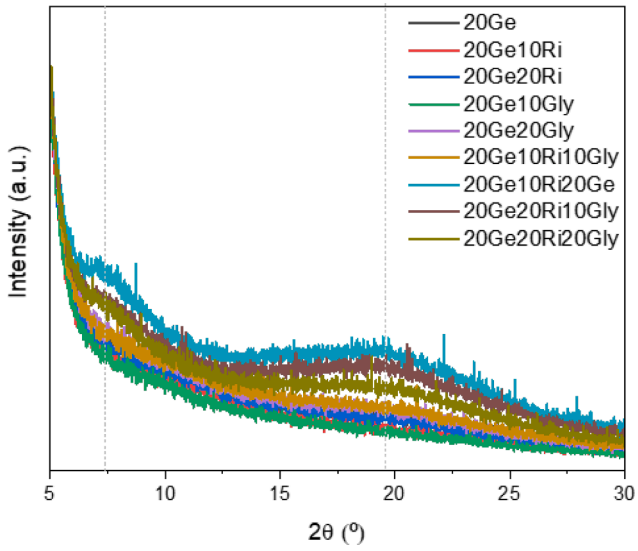

Fig. 7. XRD patterns of 20 % w/v gelatin (20Ge) mats heat-treated at 110 °C for 24 h, as a function of ribose (Ri) and glycerol (Gly) content (10 and 20 wt%, on a gelatin dry basis).

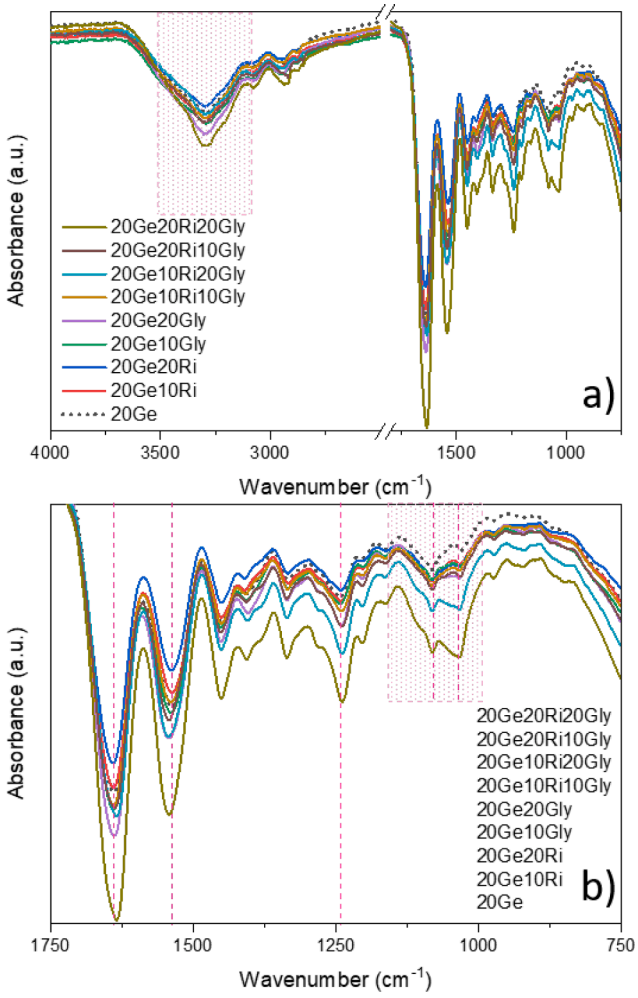

Fig. 8. FTIR spectra of 20 % w/v gelatin (20Ge) mats heat-treated at 110 °C for 24 h as a function of ribose (Ri) and glycerol (Gly) content (10 and 20 wt%, on a gelatin dry basis), a) full scale (4000–750 cm^{-1}), and b) zoomed in the 1750–750 cm^{-1} range.

at 1630 cm^{-1} (amide I), N—H bending at 1530 cm^{-1} (amide II) and C—N stretching at 1230 cm^{-1} (amide III) [34]. Regarding the additives, the main absorption bands of glycerol were due to O—H stretching at around 3290 cm^{-1} and the five bands corresponding to the vibrations of C—C bonds (850, 940 and 1000 cm^{-1}), as well as to C—O bonds (1050 and 1100 cm^{-1}) [35]. The bands associated with ribose were located between 1160 and 950 cm^{-1}. The band at approximately 1150 cm^{-1} is a characteristic vibration of a pyranose ring, and the 1200–950 cm^{-1} region is associated with C—O and C—C stretching vibrations and C—O—H, C—C—O bending vibrations [36].

The presence of glycerol into the gelatin formulation was seen through an increase in intensity of O—H stretching bands, especially in samples with 20 wt% glycerol content (Fig. 8**a**). The addition of both additives and the effect of temperature was observed *via* the intensity changes in the 1200–950 cm^{-1} region, as well as the Amide (A, I-III) bands shifts (Fig. 8**b** and Table 3). These changes in band intensities, such as variations in the two bands (1080 and 1031 cm^{-1}) situated in the saccharide region (1150–900 cm^{-1}), and the movement of the wavenumber positions (Fig. 8**b** and Table 3), have been related to structural changes that occur during the crosslinking reaction between gelatin and sugars, promoted by temperature [13,15], as well as the presence of hydrogen bonding between glycerol and gelatin [32].

Regarding the hydrolytic stability of the gelatin-based mats, the control (20Ge) and only glycerol-containing mats (20Ge10Gly, 20Ge20Gly) were entirely soluble in water (Fig. 9**a**). This indicates that the physical interactions between gelatin and glycerol were not strong enough to maintain the integrity of the mats. The addition of ribose, however, significantly reduced the solubility of samples from 100 % (20Ge, 20Ge10Gly, 20Ge20Gly) to around 16 % for 20Ge10Ri and 20Ge20Ri. This is related to crosslinking between gelatin and ribose via the MR, promoted by temperature, since the formation of high molecular weight (HMW) compounds by crosslinking protein molecules with sugar can increase the water stability of protein-saccharide systems [15]. It is worth mentioning that the solubility values did not increase as the ribose content increased from 10 to 20 wt%. Comparable outcomes for lactose-crosslinked gelatin films were observed in our previous study, where films containing 10 wt% glycerol and crosslinked with 20 and 30 wt% lactose showed similar solubility values (around 12 %), indicating that further addition of lactose did not promote additional crosslinking reactions [37]. A further decrease in solubility (around 9 %) with the addition of glycerol, especially at 20 wt% content, was observed on mats containing ribose. A similar result was seen by Ma and co-workers, where a reduction of water solubility for a gelatin film was observed as the glycerol content increased. The decrease in solubility was related to the combination of chemical and physical crosslinking, where the latter further improved the integrity of gelatin mats during immersion [38,39].

When it comes to water absorption capacity, unlike 20Ge, 20Ge10Gly and 20Ge20Gly, ribose-containing gelatin mats, regardless of glycerol content, showed water retention properties (Fig. 9**b**), which were related to the presence of chemical and physical crosslinks in the mats, as seen in FTIR and solubility results (Fig. 8 and Fig. 9**a**). These crosslinks decreased the hydrolytic degradation of gelatin, while allowing the mats to swell and maintain their integrity. Swelling values decreased as the concentration of additives increased. This reduction was related to more interactions that made for a stronger polymer network, which, in turn, hindered the water molecules' entrance into the polymer network [12]. The improvement of hydrolytic stability and water absorption ability of crosslinked gelatin mats can be considered as an advantage for the potential use of these mats in biomedical applications such as wound healing [40], and in food packaging applications such as absorbents pads for meat packaging [41], among others.

The immersion of mats in MQW can result in the migration of components (gelatin, glycerol, ribose, Maillard reaction products (MRPs)) from the sample into the liquid, and so leaching of these compounds was studied using UV–vis spectroscopy (Fig. 10**a**). Unlike the control (20Ge) and only glycerol-containing gelatin mats (20Ge10Gly, 20Ge20Gly), all 100 % water-soluble, the ribose-containing mats presented a lower migration (dissolution) of gelatin, since a narrowing in the absorption band related to peptide bonds of gelatin (200–250 nm) [42] was observed in all gelatin mats with ribose, regardless of the sugar content. This was related to the crosslinking reaction, which could reduce the dissolution of gelatin into MQW due to the formation of HMW compounds by crosslinking protein molecules. Ribose-crosslinked mats also presented a broad band between 250 and 300 nm, which was related to the release of water-soluble MRPs. It is worth mentioning that the 20Ge20Ri mats released the highest amount of MRPs, which could be related to the higher formation of these water-soluble compounds, due to the presence of a higher sugar content in the formulation. MRPs have been reported to have antioxidant activity [24,43] and so, the antioxidant properties of the released MRPs were assessed through the DPPH radical scavenging assay, and the results are shown in Fig. 10**b** and Table 3S.

Gelatin mats without ribose exhibited ~ 5 % DPPH radical scavenging capacity. This result indicated that the gelatin itself had some antioxidant effects, which could be associated with the presence of antioxidant peptide fractions [12,44]. The addition of ribose into the gelatin formulation notably increased the inhibition values of mats, and the antioxidant activity increased as the ribose content increased. However, the addition of glycerol into ribose-containing gelatin mats compromised the antioxidant properties of the samples, especially with 20Ge10Ri20Gly, 20Ge20Ri10Gly and 20Ge20Ri20Gly. The decrease of antioxidant activity of ribose-crosslinked mats containing glycerol can be related to water activity (a_w) modification or the dilution effect of glycerol (plasticizer, humectant). This could affect the formation and concentration of MRPs, since this plasticizer has been used as an a_w-adjusting agent in the MR and diluent agent [45]. Further investigation is necessary in this regard. However, the release of MRPs and their antioxidant activity can provide beneficial properties for the potential use of these mats in active food packaging, as well as in wound healing applications [46,47].

Table 3
Amide A, I, II, and III band wavenumbers for 20 % w/v gelatin (20Ge) mats heat-treated at 110 °C for 24 h as a function of ribose (Ri) and glycerol (Gly) content (10 and 20 wt%, on a gelatin dry basis). Two means followed by the same letter in the same column are not significantly ($P > 0.05$) different using Tukey's multiple range test ($n = 4$).

Gelatin mats	Amide A	Amide I	Amide II	Amide III
20Ge	3285.9 ± 3.5^{a}	1636.4 ± 1.0^{a}	1535.7 ± 3.4^{ab}	1240.6 ± 0.8^{ab}
20Ge10Ri	3291.2 ± 4.2^{ab}	1639.8 ± 5.3^{a}	1534.7 ± 5.0^{ab}	1236.3 ± 0.0^{c}
20Ge20Ri	3292.2 ± 2.0^{ab}	1637.4 ± 0.0^{a}	1531.3 ± 0.0^{a}	1242.0 ± 0.0^{b}
20Ge10Gly	3292.2 ± 2.0^{ab}	1638.4 ± 0.9^{a}	1537.6 ± 2.5^{b}	1242.0 ± 0.0^{b}
20Ge20Gly	3294.1 ± 6.4^{ab}	1641.3 ± 0.0^{a}	1544.8 ± 0.0^{c}	1238.2 ± 0.0^{bc}
20Ge10Ri10Gly	3297.5 ± 3.4^{b}	1639.8 ± 0.9^{a}	1535.2 ± 0.0^{ab}	1238.2 ± 0.0^{bc}
20Ge10Ri20Gly	3292.4 ± 1.7^{ab}	1637.4 ± 0.0^{a}	1544.8 ± 0.0^{c}	1242.0 ± 0.0^{b}
20Ge20Ri10Gly	3291.8 ± 2.4^{ab}	1630.7 ± 1.6^{b}	1534.3 ± 1.6^{ab}	1240.1 ± 2.8^{ab}
20Ge20Ri20Gly	3291.7 ± 2.1^{ab}	1629.7 ± 0.0^{b}	1535.2 ± 0.0^{ab}	1240.1 ± 0.0^{ab}

4. Conclusions

Ribose- and/or glycerol-containing electrospun gelatin-based mats were produced in this study. Gelatin solutions with concentrations ≥ 16 % w/v favoured the formation of smooth, bead-free nanofibres (diameters between 300 and 400 nm). Heat treatments at 110 and 100 °C

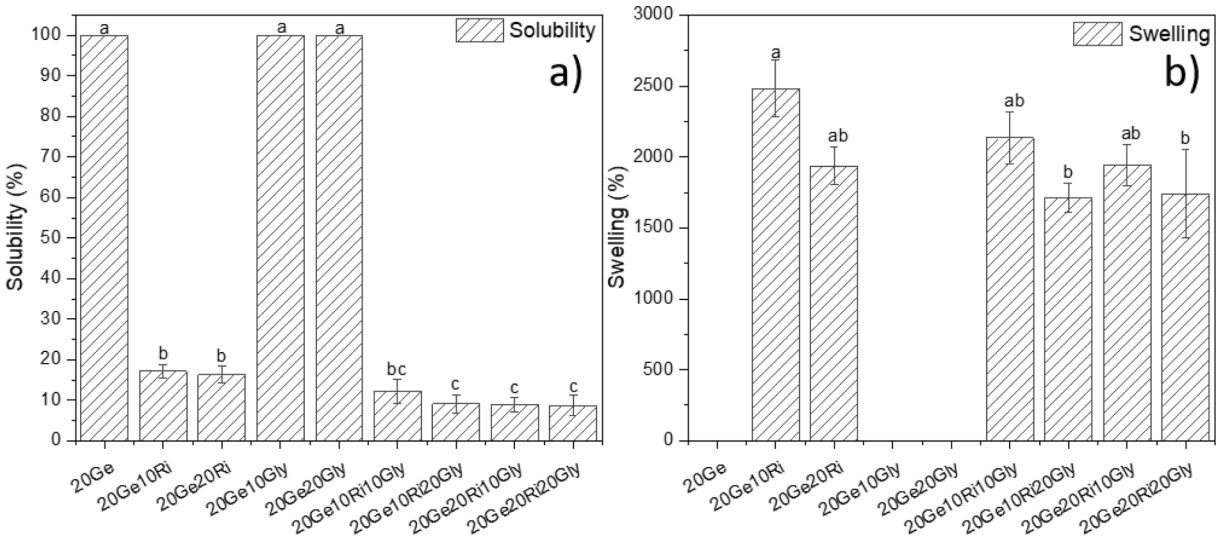

Fig. 9. a) Solubility and b) swelling values of 20 % w/v gelatin (20Ge) mats heat-treated at 110 °C for 24 h as a function of ribose (Ri) and glycerol (Gly) content (10 and 20 wt%, on a gelatin dry basis). Two means followed by the same letter are not significantly ($P > 0.05$) different using Tukey's multiple range test ($n = 3$).

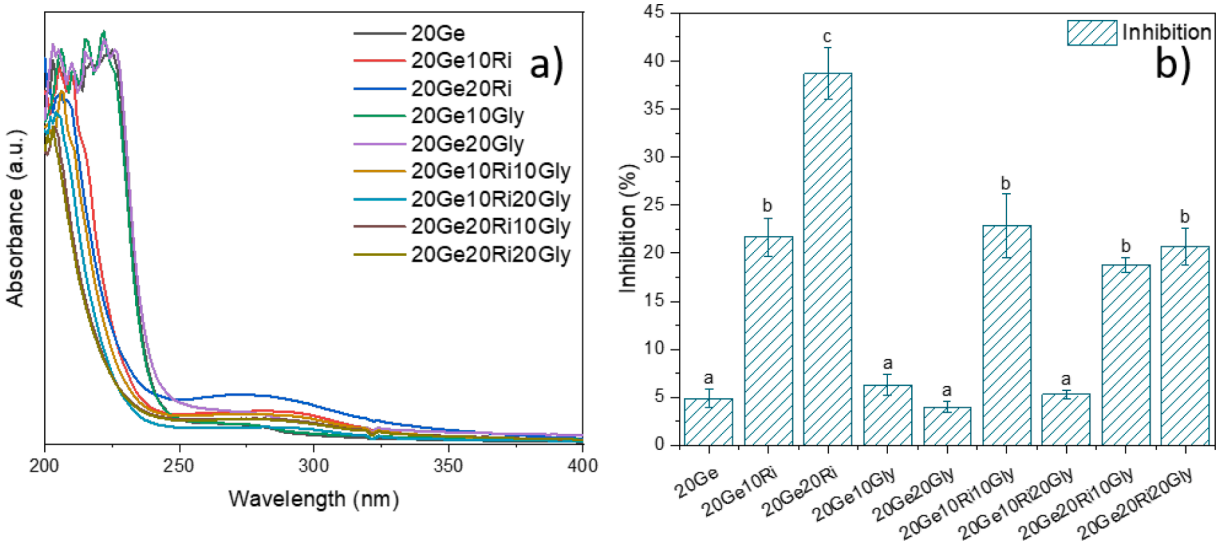

Fig. 10. a) UV–vis spectra and b) inhibition values of Maillard reaction products released from 20 % w/v gelatin (20Ge) mats heat-treated at 110 °C for 24 h as a function of ribose (Ri) and/or glycerol (Gly) content (10 and 20 wt%, on a gelatin dry basis). Two means followed by the same letter are not significantly ($P > 0.05$) different using Tukey's multiple range test ($n = 3$).

on mats containing 10 and 20 wt% ribose, respectively, provided mats with water stability and maintained a fibrous morphology after immersion, due to crosslinking between gelatin and ribose known as the Maillard reaction (MR). Heat treatment at 110 °C and the addition of glycerol resulted in a decrease of solubility and provided mats with water absorption capacity as well as antioxidant activity due to the presence of a chemical and a physical (hydrogen bonding) crosslinking induced by ribose and glycerol with gelatin. This study shows that i) gelatin was successfully electrospun using only water as a solvent, and ii) the Maillard reaction, and the addition of glycerol in gelatin formulations, are viable alternatives to improve and tailor the functional properties of electrospun gelatin mats for active food packaging and wound healing applications.

CRediT authorship contribution statement

Alaitz Etxabide: Conceptualization, Methodology, Validation, Investigation, Writing – original draft, Writing – review & editing. **Alireza Akbarinejad:** Investigation, Writing – review & editing. **Eddie W.C. Chan:** Investigation, Writing – review & editing. **Pedro Guerrero:** Writing – review & editing, Supervision. **Koro de la Caba:** Writing – review & editing, Supervision, Funding acquisition. **Jadranka Travas-Sejdic:** Conceptualization, Writing – review & editing, Supervision. **Paul A. Kilmartin:** Writing – review & editing, Supervision, Funding acquisition.

Declaration of Competing Interest

The authors declare that they have no known competing financial interests or personal relationships that could have appeared to influence the work reported in this paper.

Data availability

No data was used for the research described in the article.

Acknowledgement

The authors would like to thank the Ministry of Business, Innovation and Employment of New Zealand (MBIE, Biocide Toolbox programme) and the Basque Government (IT1658-22) for funding. A.E. thanks the State Research Agency of Spain within the Juan de la Cierva - Incorporation action (IJC2019-039697I).

Data availability

Data sharing not applicable.

Appendix A. Supplementary data

Supplementary data to this article can be found online at https://doi.org/10.1016/j.eurpolymj.2022.111597.

References

[1] S. Tan, R. Inai, M. Kotaki, S. Ramakrishna, Systematic parameter study for ultra-fine fiber fabrication via electrospinning process, 46 (2005) 6128-6134. https://doi.org/10.1016/j.polymer.2005.05.068.
[2] E. Kny, K. Ghosal, S. Thomas, Electrospinning: From Basic Research to Commercialization, The Royal Society of Chemistry, 2018.
[3] N. Okutan, P. Terzi, F. Altay, Affecting parameters on electrospinning process and characterization of electrospun gelatin nanofibers, Food Hydrocoll. 39 (2014) 19–26, https://doi.org/10.1016/j.foodhyd.2013.12.022.
[4] J. Xue, T. Wu, Y. Dai, Y. Xia, Electrospinning and electrospun nanofibers: Methods, materials, and applications, Chem. Rev. 119 (8) (2019) 5298–5415, https://doi.org/10.1021/acs.chemrev.8b00593.
[5] Thomas Kerr-Phillips, Jadranka Travas-Sejdic, Conducting Polymers: Electrospun Materials, in: Munmaya Mishra (Ed.), Encyclopedia of Polymer Applications, CRC Press, Taylor and Francis, 2019, pp. 602-623.
[6] E.W.C. Chan, D. Bennet, P. Baek, D. Barker, S. Kim, J. Travas-Sejdic, Electrospun Polythiophene Phenylenes for Tissue Engineering, 19 (2018) 1456-1468. https://doi.org/10.1021/acs.biomac.8b00341.
[7] S. Beikzadeh, A. Akbarinejad, S. Swift, J. Perera, P.A. Kilmartin, J. Travas-Sejdic, Cellulose acetate electrospun nanofibers encapsulating Lemon Myrtle essential oil as active agent with potent and sustainable antimicrobial activity, React Funct Polym. 157 (2020) 104769, https://doi.org/10.1016/j.reactfunctpolym.2020.104769.
[8] A. Contreras, M.J. Raxworthy, S. Wood, G. Tronci, Hydrolytic degradability, cell tolerance and on-demand antibacterial effect of electrospun photodynamically active fibres, Pharmaceutics 12 (2020) 711, https://doi.org/10.3390/pharmaceutics12080711.
[9] J.L. Hernandez, M.A. Doan, R. Stoddard, H.M. VanBenschoten, S.T. Chien, I. T. Suydam, K.A. Woodrow, Scalable electrospinning methods to produce high basis weight and uniform drug eluting fibrous biomaterials, Front. Front. Biomater. Sci. 1 (2022), 928537, https://doi.org/10.3389/fbiom.2022.928537.
[10] D. Lv, M. Zhu, Z. Jiang, S. Jiang, Q. Zhang, R. Xiong, et al, Green Electrospun Nanofibers and Their Application in Air Filtration, Macromol.Mater.Eng. 303 (2018) 1800336. https://doi.org/10.1002/mame.201800336.
[11] G. S. Krishnakumar, S. Sampath, S. Muthusamy, M. A. John, Importance of crosslinking strategies in designing smart biomaterials for bone tissue engineering: A systematic review, 96 (2019) 941-954. https://doi.org/10.1016/j.msec.2018.11.081.
[12] H.W. Kwak, J. Park, H. Yun, K. Jeon, D.-W. Kang, Effect of crosslinkable sugar molecules on the physico-chemical and antioxidant properties of fish gelatin nanofibers, Food Hydrocoll. 111 (2021) 106259, https://doi.org/10.1016/j.foodhyd.2020.106259.
[13] H. Kchaou, N. Benbettaïeb, M. Jridi, O. Abdelhedi, T. Karbowiak, C.-H. Brachais, M.-L. Léonard, F. Debeaufort, M. Nasri, Enhancement of structural, functional and antioxidant properties of fish gelatin films using Maillard reactions, Food Hydrocoll. 83 (2018) 326–339, https://doi.org/10.1016/j.foodhyd.2018.05.011.
[14] A. Etxabide, C. Vairo, E. Santos-Vizcaino, P. Guerrero, J.L. Pedraz, M. Igartua, K. de la Caba, R.M. Hernandez, Ultra thin hydro-films based on lactose-crosslinked fish gelatin for wound healing applications, Int. J. Pharm. 530 (1-2) (2017) 455–467, https://doi.org/10.1016/j.ijpharm.2017.08.001.
[15] A. Etxabide, P.A. Kilmartin, J.I. Maté, S. Prabakar, M. Brimble, R. Naffa, Analysis of Advanced Glycation End products in ribose-, glucose- and lactose-crosslinked gelatin to correlate the physical changes induced by Maillard reaction in films, Food Hydrocoll. 117 (2021) 106736, https://doi.org/10.1016/j.foodhyd.2021.106736.
[16] R. ter Haar, H.A. Schols, H. Gruppen, Effect of saccharide structure and size on the degree of substitution and product dispersity of α-lactalbumin glycated via the maillard reaction, J. Agric Food Chem. 59 (17) (2011) 9378–9385, https://doi.org/10.1021/jf2027395.
[17] G.B. Naranjo, A.S. Pereyra Gonzales, G.E. Leiva, L.S. Malec, The kinetics of Maillard reaction in lactose-hydrolysed milk powder and related systems containing carbohydrate mixtures, Food Chem. 141 (4) (2013) 3790–3795, https://doi.org/10.1016/j.foodchem.2013.06.093.
[18] A. Etxabide, M. Urdanpilleta, I. Gómez-Arriaran, K. de la Caba, P. Guerrero, Effect of pH and lactose on cross-linking extension and structure of fish gelatin films, React Funct Polym. 117 (2017) 140–146, https://doi.org/10.1016/j.reactfunctpolym.2017.04.005.
[19] M. Stevenson, J. Long, A. Seyfoddin, P. Guerrero, K.d.l. Caba, A. Etxabide, Characterization of ribose-induced crosslinking extension in gelatin films, Food Hydrocoll. 99 (2020) 105324, https://doi.org/10.1016/j.foodhyd.2019.105324.
[20] F.A. Osorio, E. Bilbao, R. Bustos, F. Alvarez, Effects of concentration, bloom degree, and pH on gelatin melting and gelling temperatures using small amplitude oscillatory rheology, Int. J. Food Prop. 10 (4) (2007) 841–851, https://doi.org/10.1080/10942910601128895.
[21] J.M. Peralta, B.E. Meza, S.E. Zorrilla, Analytical solutions for the free-draining flow of a Carreau-Yasuda fluid on a vertical plate, 168 (2017) 391-402. https://doi.org/10.1016/j.ces.2017.05.002.
[22] P. Sajkiewicz, D. Kołbuk, Electrospinning of gelatin for tissue engineering – molecular conformation as one of the overlooked problems, 25 (2014) 2009-2022. https://doi.org/10.1080/09205063.2014.975392.
[23] A. Etxabide, M. Urdanpilleta, P. Guerrero, K. de la Caba, Effects of cross-linking in nanostructure and physicochemical properties of fish gelatins for bio-applications, React Funct Polym. 94 (2015) 55–62, https://doi.org/10.1016/j.reactfunctpolym.2015.07.006.
[24] A. Etxabide, P.A. Kilmartin, J.I. Maté, J. Gómez-Estaca, Characterization of glucose-crosslinked gelatin films reinforced with chitin nanowhiskers for active packaging development, 154 (2022) 112833. https://doi.org/10.1016/j.lwt.2021.112833.
[25] E. Hoch, C. Schuh, T. Hirth, G.E.M. Tovar, K. Borchers, Stiff gelatin hydrogels can be photo-chemically synthesized from low viscous gelatin solutions using molecularly functionalized gelatin with a high degree of methacrylation, J. Mater. Sci. Mater. Med. 23 (11) (2012) 2607–2617, https://doi.org/10.1007/s10856-012-4731-2.
[26] J. Enrione, C. Char, M. Pepczynska, C. Padilla, A. González-Muñoz, Y. Olguín, C. Quinzio, L. Iturriaga, P. Díaz-Calderón, Rheological and structural study of salmon gelatin with controlled molecular weight, Polymers. 12 (7) (2020) 1587, https://doi.org/10.3390/polym12071587.
[27] J.L. Gornall, E.M. Terentjev, Helix-coil transition of gelatin: helical morphology and stability, Soft Matter 4 (2008) 544–549, https://doi.org/10.1039/b713075a.
[28] A.L. Ellis, T.B. Mills, I.T. Norton, A.B. Norton-Welch, The effect of sugars on agar fluid gels and the stabilisation of their foams, Food Hydrocoll. 87 (2019) 371–381, https://doi.org/10.1016/j.foodhyd.2018.08.027.
[29] B. Tarus, N. Fadel, A. Al-Oufy, M. El-Messiry, Effect of polymer concentration on the morphology and mechanical characteristics of electrospun cellulose acetate and poly (vinyl chloride) nanofiber mats, 55 (2016) 2975-2984. https://doi.org/10.1016/j.aej.2016.04.025.
[30] K. Siimon, P. Reemann, A. Põder, M. Pook, T. Kangur, K. Kingo, et al, Effect of glucose content on thermally cross-linked fibrous gelatin scaffolds for tissue engineering, 42 (2014) 538-545. https://doi.org/10.1016/j.msec.2014.05.075.
[31] R. Gharaei, G. Tronci, R.P.W. Davies, C. Gough, R. Alazragi, P. Goswami, S. J. Russell, A structurally self-assembled peptide nano-architecture by one-step electrospinning, J. Mater. Chem. B 4 (32) (2016) 5475–5485, https://doi.org/10.1039/C6TB01164K.
[32] R. Morsy, M. Hosny, F. Reicha, T. Elnimr, Developing and physicochemical evaluation of cross-linked electrospun gelatin–glycerol nanofibrous membranes for medical applications, J. Mol. Struct. 1135 (2017) 222–227.
[33] F. Liu, J. Antoniou, Y. Li, J. Ma, F. Zhong, Effect of sodium acetate and drying temperature on physicochemical and thermomechanical properties of gelatin films, Food Hydrocoll. 45 (2015) 140–149, https://doi.org/10.1016/j.foodhyd.2014.10.009.
[34] S.D. Frazier, W.V. Srubar, Evaporation-based method for preparing gelatin foams with aligned tubular pore structures, 62 (2016) 467-473. https://doi.org/10.1016/j.msec.2016.01.074.
[35] H. Ren, C. Cai, C. Leng, S. Pang, Y. Zhang, Nucleation Kinetics in Mixed NaNO3/Glycerol Droplets Investigated with the FTIR–ATR Technique, J. Phys. Chem. B. 120 (2016) 2913-2920. https://doi.org/10.1021/acs.jpcb.5b12442.
[36] Y. Lu, J. Guo, Metal-ion interactions with sugars. Crystal structure and FT-IR study of PrCl3–d-ribose complex, Carbohydr. Res. 341 (5) (2006) 683–687, https://doi.org/10.1016/j.carres.2005.12.011.
[37] A. Etxabide, J. Uranga, P. Guerrero, K. de la Caba, Improvement of barrier properties of fish gelatin films promoted by gelatin glycation with lactose at high temperatures, 63 (2015) 315-321. https://doi.org/10.1016/j.lwt.2015.03.079.
[38] L. Ma, H. Yang, M. Ma, X. Zhang, Y. Zhang, Mechanical and structural properties of rabbit skin gelatin films, Int. J. Food Prop. 21 (1) (2018) 1203–1218, https://doi.org/10.1080/10942912.2018.1476874.
[39] A. Parak, P. Pradeep, L.C. du Toit, P. Kumar, Y.E. Choonara, V. Pillay, Functionalizing bioinks for 3D bioprinting applications, Drug Discov. Today. 24 (1) (2019) 198–205, https://doi.org/10.1016/j.drudis.2018.09.012.
[40] T. S. Vo, Vo, Tran Thi Bich Chau, T. S. Nguyen, N. D. Pham, Incorporation of hydroxyapatite in crosslinked gelatin/chitosan/poly(vinyl alcohol) hybrids utilizing as reinforced composite sponges, and their water absorption ability, 31 (2021) 664-671. https://doi.org/10.1016/j.pnsc.2021.09.003.
[41] K. K. Gaikwad, S. Singh, A. Ajji, Moisture absorbers for food packaging applications, 17 (2019) 609-628. https://doi.org/10.1007/s10311-018-0810-z.
[42] J. Bonilla, P.J.A. Sobral, Investigation of the physicochemical, antimicrobial and antioxidant properties of gelatin-chitosan edible film mixed with plant ethanolic

extracts, Food Bioscience 16 (2016) 17–25, https://doi.org/10.1016/j.fbio.2016.07.003.
[43] Y. Yilmaz, R. Toledo, Antioxidant activity of water-soluble Maillard reaction products, Food Chem. 93 (2) (2005) 273–278, https://doi.org/10.1016/j.foodchem.2004.09.043.
[44] B. Giménez, J. Gómez-Estaca, A. Alemán, M.C. Gómez-Guillén, M.P. Montero, Improvement of the antioxidant properties of squid skin gelatin films by the addition of hydrolysates from squid gelatin, Food Hydrocoll. 23 (5) (2009) 1322–1327, https://doi.org/10.1016/j.foodhyd.2008.09.010.
[45] M. Saltmarch, T. P. Labuza, Nonenzymatic Browning via the Maillard Reaction in Foods, 31 (1982) 29-36. https://doi.org/10.2337/diab.31.3.S29.
[46] I. Comino-Sanz, M. D. López-Franco, B. Castro, P. Pancorbo-Hidalgo, The Role of Antioxidants on Wound Healing: A Review of the Current Evidence, 10 (2021) 3558. https://doi.org/10.3390/jcm10163558.
[47] H. Almasi, M. Jahanbakhsh Oskouie, A. Saleh, A review on techniques utilized for design of controlled release food active packaging, Crit. Rev. Food Sci. Nutr. 61 (15) (2021) 2601–2621, https://doi.org/10.1080/10408398.2020.1783199.